Journal of Alloys and Compounds 330–332 (2002) 389–392

Journal of ALLOYS AND COMPOUNDS

www.elsevier.com/locate/jallcom

# Feasibility study of high-strength and high-damping materials by means of hydrogen internal friction in amorphous alloys

H. Mizubayashi*, S. Murayama, H. Tanimoto

*Institute of Materials Science, University of Tsukuba, Tsukuba, Ibaraki 305-8573, Japan*

**Abstract**

Exploring the feasibility of high-strength and high-damping materials, we investigated the hydrogen internal friction peak (HIFP) in amorphous (a-) $Zr_{60}Cu_{40-x}Al_x$ ($x$=0, 5, 10) and a-$Zr_{40}Cu_{50}Al_{10}$ and the tensile strength, $\sigma_f$, of a-$Zr_{60}Cu_{30}Al_{10}$ as a function of the hydrogen concentration. Results are discussed relative to the HIFP reported in a-$Zr_{50}Cu_{50}$, a-$Zr_{40}Cu_{60}$ and a-$Ti_{50}Cu_{50}$. $\sigma_f$ of a-$Zr_{60}Cu_{30}Al_{10}$ increases from 1.5 GPa in the no-charged state to 2 GPa at about 15 at.% H. The HIFP in the a-alloys is observed as a very broad peak, where the peak temperature found varies from 350 K in a-$Zr_{40}Cu_{60-x}Al_x$ with 1 at.% H to 200 K in a-$Ti_{50}Cu_{50}$ with 15 at.%. Although the HIFP with the peak height, $Q^{-1}_{peak}$, beyond $3\times10^{-2}$ is observed in a-$Zr_{60}Cu_{40-x}Al_x$ ($x$=0, 10) in the as charged state, its $Q^{-1}_{peak}$ shows a decrease after aging at 350 K due to the hydrogen induced structural relaxation (HISR). However, for all the present a-alloys, $Q^{-1}_{peak}$ observed in the thermally stable state after the HISR can be still as high as $2\times10^{-2}$. The present results suggest that the hydrogen-charged a-alloys are potential high-strength and high-damping materials. 

*Keywords:* High-damping material; Hydrogen internal friction peak; Amorphous alloy

## 1. Introduction

Future space development projects may demand smart structural materials such as a high-strength and high-damping material working near and below room temperature (RTs). The demand for such a material working near and above RT may be even more urgent for smart precision machinery, e.g. a wire bonding machine. Fig. 1 shows a specific damping index or internal friction vs. tensile strength map, where various metallic materials are classified into three groups, the high-, intermediate- and low-damping materials. The three lines are drawn to guide eyes. As indicated by a dashed-line box in Fig. 1, high-damping materials with tensile strength beyond 1 GPa may represent targets for future smart structural materials. It is known that most of amorphous (a-) alloys show the mechanical responses such as high strength, large elastic strain and low Young's modulus, indicating that they are tough and flexible. However, the internal friction, $Q^{-1}$, in a-alloys below the glass transition temperature is as low as that in the low- or intermediate-damping materials. Meanwhile since the hydrogen internal friction peak (HIFP) in a-alloys was found by Berry et al. [1], much effort has been devoted to the subject. Pronounced HIFP can be

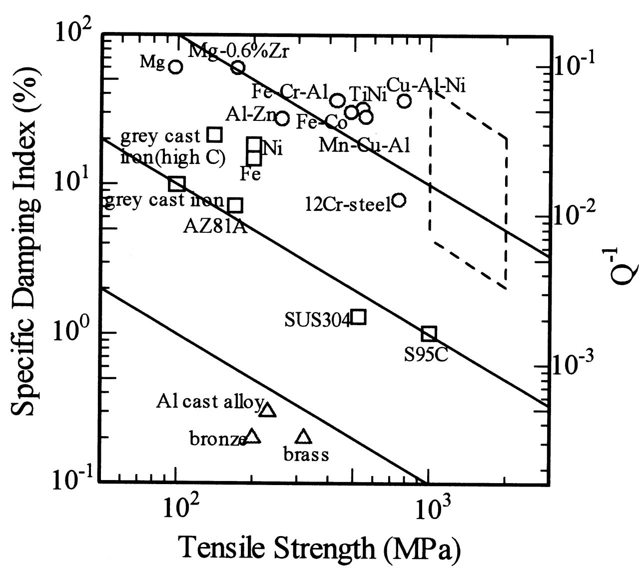


Fig. 1. A specific damping index or internal friction ($Q^{-1}$) vs. tensile strength map. The 'specific damping index' is the ratio of the energy dissipated to the maximum stored energy when expressed as a percentage.

*Corresponding author. Tel.: +81-298-535-063; fax: +81-298-557-440.

*E-mail address:* mizuh@ims.tsukuba.ac.jp (H. Mizubayashi).

0925-8388/02/$ – see front matter 
PII: S0925-8388(01)01529-8

observed in the a-alloys which can contain much hydrogen in solution [2–12]. A recent work on hydrogen-charged a-Ti–Cu and a-Zr–Cu indicates that the local strain around hydrogen in the a-alloys is highly anisotropic [13], providing the evidence that the stress-induced redistribution of hydrogen [2–12] gives rise the HIFP in a-alloys. After these works, one can expect that a hydrogen-charged a-alloys may serve us as useful high-strength and high-damping material especially by controlling the behavior of hydrogen atoms in a-alloys. The present work is the first attempt of this concept where we have examined a-Zr–Cu and a-Zr–Cu–Al alloys.

## 2. Experimental

Amorphous (a-) Zr–Cu and Zr–Cu–Al alloy ribbons about 30 μm thick and 1 mm wide were prepared by melt spinning in a high-purity Ar gas atmosphere and checked by the conventional $\theta$–$2\theta$ scan X-ray diffraction. Hydrogen charging was made electrolytically and the hydrogen concentration, $C_H$, in a hydrogen-charged specimen was measured by means of the thermal degassing method in a high vacuum. The internal friction, $Q^{-1}$, was measured by means of the vibrating reed method working at about 200 Hz and strain amplitude of $10^{-6}$.

## 3. Results and discussion

Fig. 2a shows examples of the tensile tests of a-$Zr_{60}Cu_{30}Al_{10}$ specimens at RT before or after hydrogen charging. It is noted that a-$Zr_{60}Cu_{30}Al_{10}$ is known as one of the high glass-forming-ability a-alloys [14]. Fig. 2b shows the fracture strength, $\sigma_f$, found in Fig. 2(a). $\sigma_f$ observed for the as-prepared specimens is 1.5 GPa and shows an increase to 2 GPa with increasing $C_H$ in the present $C_H$ range, indicating that the prerequisite for $\sigma_f$ mentioned in Fig. 1 is satisfied for $C_H$ below 15 at.%.

Fig. 3a shows examples of the HIFP observed in as-quenched a-$Zr_{60}Cu_{30}Al_{10}$ specimens with $C_H$ below 15 at.%. The specimen with 4.5 at.% H has been annealed at 600 K for 2 h in a vacuum prior to hydrogen charging. Fig. 3b is similar to Fig. 3a but for the HIFP observed in as-quenched a-$Zr_{40}Cu_{50}Al_{10}$ specimens with $C_H$ below 16 at.%. For the sake of simplicity, only the heating runs are shown except that both the heating and cooling runs are shown for a couple of specimens as indicated in Fig. 3a and b. Both the HIFP in a-$Zr_{60}Cu_{30}Al_{10}$ specimens and that in a-$Zr_{40}Cu_{50}Al_{10}$ specimens are observed as a very broad peak similar to the HIFP in a-$Zr_{50}Cu_{50}$ [11] or a-$Zr_{40}Cu_{60}$ [15]. In the following, we shall characterize the HIFP by the peak temperature, $T_{peak}$, and peak height, $Q^{-1}_{peak}$. As seen in Fig. 3a, $T_{peak}$ observed in a-$Zr_{60}Cu_{30}Al_{10}$ is about 280 K in the specimen with 1.1 at.% H and shows a decrease down to about 250 K with

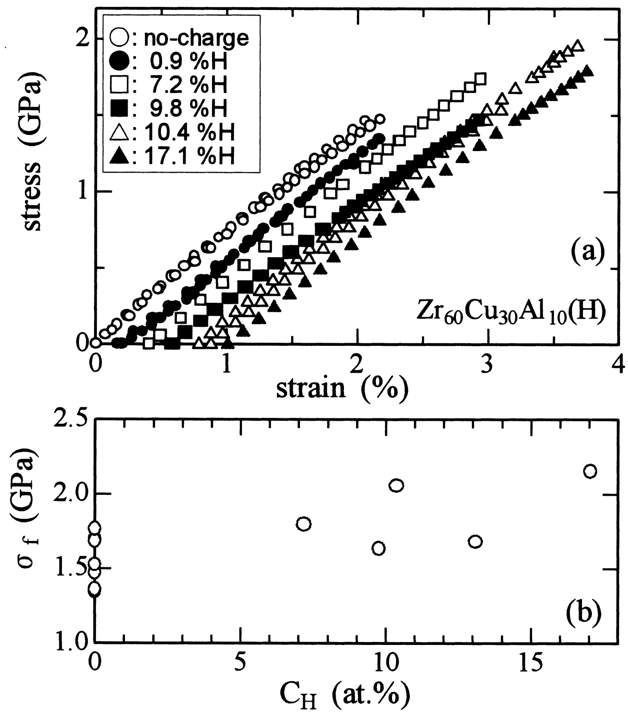


Fig. 2. (a) Examples of the tensile tests of a-$Zr_{60}Cu_{30}Al_{10}$ specimens at RT before or after hydrogen charging. (b) The fracture strength, $\sigma_f$, found in (a).

increasing $C_H$. On the other hand, as seen in Fig. 3b, $T_{peak}$ found in a-$Zr_{40}Cu_{50}Al_{10}$ is about 350 K in the specimen with 1.3 at.% H and shows a decrease down to about 250

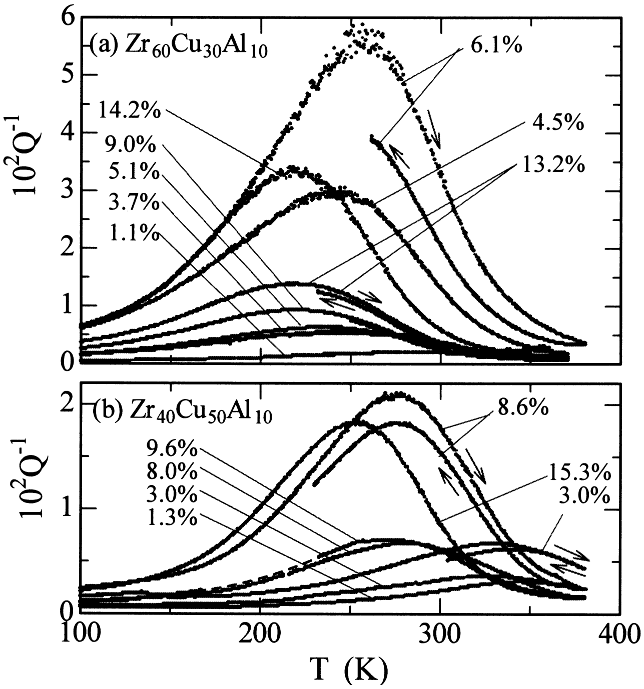


Fig. 3. (a) Examples of the HIFP observed in a-$Zr_{60}Cu_{30}Al_{10}$ specimens. (b) Examples of the HIFP observed in a-$Zr_{40}Cu_{50}Al_{10}$ specimens. See text for details.

K with increasing $C_H$. That is, $T_{peak}$ found in the low $C_H$ range is higher in a-$Zr_{40}Cu_{50}Al_{10}$ than in a-$Zr_{60}Cu_{30}Al_{10}$. For $Q^{-1}_{peak}$, the HIFP with $Q^{-1}_{peak}$ beyond $3\times10^{-2}$ can be observed in a-$Zr_{60}Cu_{30}Al_{10}$ and in contrast, $Q^{-1}_{peak}$ observed in a-$Zr_{40}Cu_{50}Al_{10}$ remains near or below $2\times10^{-2}$. These issues will be mentioned later. For the heating and cooling runs shown in Fig. 3a and b, a decrease in $Q^{-1}_{peak}$ after heating up to about 380 K is observed for the as charged specimen. The decrease in $Q^{-1}_{peak}$ is not due to degassing of hydrogen but due to the structural relaxation. The higher the $Q^{-1}_{peak}$ is, the larger the decrease in $Q^{-1}_{peak}$ is. This observed result again suggests that the anisotropic local strain around hydrogen in the a-alloys is responsible for both the HIFP [13] and the hydrogen induced structural relaxation (HISR) in a-alloys [15].

Fig. 4 shows the $T_{peak}$ vs. $C_H$ data found for various a-alloys. The general trend of a decrease in $T_{peak}$ with increasing $C_H$ is believed to reflect an increase in the chemical potential of hydrogen in a-alloys with increasing $C_H$ [3,16,17]. As seen in Fig. 4, $T_{peak}$ found at $C_H$ near 1 at.% is about 280 K for a-$Zr_{50}Cu_{50}$, a-$Zr_{60}Cu_{40-x}Al_x$ ($x=0$, 5, 10) and a-$Ti_{50}Cu_{50}$ and about 350 K for a-$Zr_{40}Cu_{60-x}Al_x$ ($x=0$, 10), suggesting that the representative activation enthalpy of hydrogen migration at the low $C_H$ range is higher in a-$Zr_{40}Cu_{60-x}Al_x$ than in the other a-alloys. In later-transition-metal/early-transition-metal a-alloy, a-$A_yB_{1-y}$, the maximum hydrogen content in the $A_mB_{4-m}$ sites, $\Delta C_{y,m}$, may be given by:

$$\Delta C_{y,m} = f_0[4!/m!(4-m)!]\cdot y^m \cdot (1-y)^{4-m} \quad (1)$$

where the alloys are assumed to be structurally isomorphic and chemically random and $f_0=1.6$ at $y=0.5$ [18]. Eq. (1) predicts that most of hydrogen atoms may occupy the $Zr_4$ (or $Ti_4$) sites in the $C_H$ range below about 20 at.% for a-$Zr_{60}Cu_{40-x}Al_x$, below about 10 at.% for a-$Zr_{50}Cu_{50}$ and a-$Ti_{50}Cu_{50}$ and below about 4 at.% for a-$Zr_{40}Cu_{60-x}Al_x$. This suggests that the HIFP observed near 1 at.% H may associated with the stress-induced redistribution of hydrogen atoms which are sitting in the $Zr_4$ (or $Ti_4$) sites. The fact that the HIFP in a-alloys is observed as a very broad peak suggests that the redistribution of hydrogen atoms may take place by migration of hydrogen atoms threading through various tetrahedral sites. We assume below the representative migration path of hydrogen atoms which is responsible for $T_{peak}$. Eq. (1) also predicts that $\Delta C_{y,0}$ for the (Cu and/or Al)$_4$ sites is about 20 at.% in a-$Zr_{40}Cu_{60-x}Al_x$, about 10 at.% for a-$Zr_{50}Cu_{50}$ and a-$Ti_{50}Cu_{50}$ and about 4 at.% for a-$Zr_{60}Cu_{40-x}Al_x$, respectively. After the consideration mentioned above, we surmise that the representative migration path of hydrogen atoms responsible for $T_{peak}$ inevitably threads through the (Cu and/or Al)$_4$ sites in a-$Zr_{40}Cu_{60-x}Al_x$ but it is not the case in a-$Zr_{50}Cu_{50}$, a-$Zr_{60}Cu_{40-x}Al_x$ ($x=0$, 5, 10) and a-$Ti_{50}Cu_{50}$. In other words, the present results indicate that $T_{peak}$ can be controlled in between 350 and 250 K by adjusting composition of a-alloys.

Fig. 5a–d show the $Q^{-1}_{peak}$ vs. $C_H$ data observed for various a-alloys. As seen in Fig. 5a, as-hydrogen-charged a-$Zr_{60}Cu_{40-x}Al_x$ specimens can be classified into two groups, the specimens showing $Q^{-1}_{peak}$ beyond $3\times10^{-2}$ and those showing $Q^{-1}_{peak}$ below $2\times10^{-2}$. It is noted that no changes in the X-ray diffraction spectra are detected among these specimens. As already seen in Fig. 3a, $Q^{-1}_{peak}$ beyond $3\times10^{-2}$ are also found in the specimens which were annealed at 600 K before hydrogen charging. In

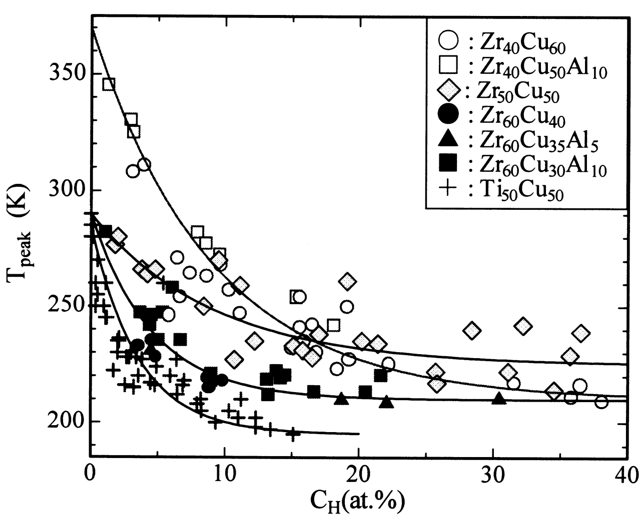


Fig. 4. The $T_{peak}$ vs. $C_H$ data found for various a-alloys, where the data found in a-$Ti_{50}Cu_{50}$ [10], a-$Zr_{50}Cu_{50}$ [11] and a-$Zr_{40}Cu_{60}$ [15] are also shown.

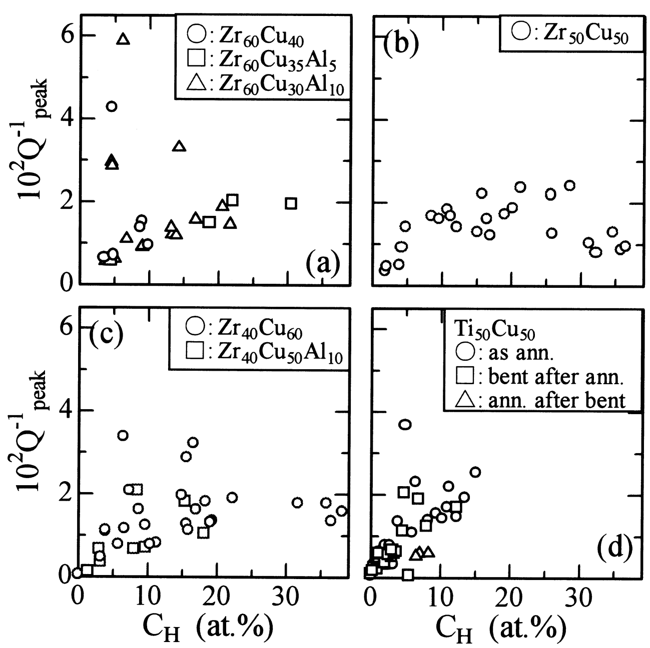


Fig. 5. The $Q^{-1}_{peak}$ vs. $C_H$ data observed; (a) a-$Zr_{60}Cu_{40-x}Al_x$, (b) a-$Zr_{50}Cu_{50}$ [11], (c) a-$Zr_{40}Cu_{60}$ [15] and a-$Zr_{40}Cu_{50}Al_{10}$ and (d) a-$Ti_{50}Cu_{50}$ [10].

contrast, no specimens showing $Q^{-1}_{peak}$ beyond $3\times10^{-2}$ are found for the specimens which were annealed at 350 K for 1 day after hydrogen charging (not shown here), suggesting that the HISR takes place in a-$Zr_{60}Cu_{30}Al_{10}$ as well as in a-$Zr_{40}Cu_{60}$ [15]. As seen in Fig. 3a and b, the decrease in $Q^{-1}_{peak}$ due to the HISR is much smaller for the HIFP with $Q^{-1}_{peak}$ below $2\times10^{-2}$ than for the HIFP with $Q^{-1}_{peak}$ beyond $3\times10^{-2}$, indicating that the former reflects the HIFP in the thermally stable state. For a-$Zr_{60}Cu_{30}Al_{10}$, the $Q^{-1}_{peak}$ data found below $2\times10^{-2}$ show an increase in $Q^{-1}_{peak}$ followed by saturation with increasing $C_H$. For a-$Zr_{50}Cu_{50}$ shown in Fig. 5b, the $Q^{-1}_{peak}$ data are found below $3\times10^{-2}$, where the $Q^{-1}_{peak}$ vs. $C_H$ data show two humps which are assumed to reflect the hydrogen-site-energy distribution in the a-alloy [11]. The outline of the $Q^{-1}_{peak}$ vs. $C_H$ data observed in a-$Zr_{40}Cu_{60-x}Al_x$ specimens shown in Fig. 5c and that in a-$Ti_{50}Cu_{50}$ specimens shown in Fig. 5d are similar to that seen for a-$Zr_{60}Cu_{30}Al_{10}$ specimens. It is noted that as seen in Fig. 5d [10] or reported in [19], plastic deformation of an a-alloy specimen modifies the HIFP, however this issue is out of the present scope. After Fig. 5a–d, we can say that $Q^{-1}_{peak}$ of the present a-alloys in the thermally stable state can be as high as $2\times10^{-2}$, suggesting that the prerequisite for $Q^{-1}_{peak}$ mentioned in Fig. 1 may be satisfied by adjusting composition of a-alloys.

## 4. Conclusion

We investigated the HIFP in a-$Zr_{60}Cu_{40-x}Al_x$ ($x=0$, 5, 10) and a-$Zr_{40}Cu_{50}Al_{10}$ and $\sigma_f$ of a-$Zr_{60}Cu_{30}Al_{10}$ as a function of $C_H$ and discussed them together with the HIFP in a-$Zr_{50}Cu_{50}$, a-$Zr_{40}Cu_{60}$ and a-$Ti_{50}Cu_{50}$ previously reported. $\sigma_f$ of a-$Zr_{60}Cu_{30}Al_{10}$ increases from 1.5 GPa at 0 at.% H to 2 GPa at about 15 at.% H. The peak temperature found varies from 350 K in a-$Zr_{40}Cu_{60-x}Al_x$ with 1 at.% H to 200 K in a-$Ti_{50}Cu_{50}$ with 15 at.%. $Q^{-1}_{peak}$ observed in the present a-alloys in the thermally stable state can be as high as $2\times10^{-2}$. From these results, we can say that the hydrogen charged a-alloys are potential materials in view of a high-strength and high-damping material. However, tuning the specimen conditions up is required further.

## Acknowledgements

This work is partly supported by 'New Protium Function in Sub-Nano Lattice Matters' research project of a Grant in Aid for Scientific Research from the Ministry of Education, Science and Culture of Japan, and High Damping Materials Project of 'Research for the Future' of Japan Society for the Promotion of Science.

## References

[1] B.S. Berry, W.C. Pritchet, C.C. Tsuei, Phys. Rev. Lett. 41 (1978) 410.
[2] H.-U. Kunzi, K. Agyeman, H.-J. Guntherodt, Solid State Commun. 32 (1979) 711.
[3] B.S. Berry, W.C. Pritchet, J. Phys. 42 (1981) C5–1111.
[4] O. Yoshinari, M. Koiwa, A. Inoue, T. Masumoto, Acta Metall. 31 (1983) 2063.
[5] U. Stolz, M. Weller, R. Kirchheim, Scripta Metall. 20 (1986) 1361.
[6] H. Mizubayashi, Y. Katoh, S. Okuda, Phys. Stat. Sol. (a) 104 (1988) 469.
[7] B.S. Berry, W.C. Pritchet, in: G. Bambakidis, R.C. Bowman Jr. (Eds.), Hydrogen in Disordered and Amorphous Solids, Plenum Press, 1986, p. 215.
[8] U. Stolz, J. Phys. F 17 (1987) 1833.
[9] B.S. Berry, W.C. Pritchet, Z. Phys. Chem. Neue Folge 163 (1989) 381.
[10] H. Mizubayashi, H. Agari, S. Okuda, Phys. Stat. Sol. (a) 122 (1990) 221.
[11] H. Mizubayashi, T. Naruse, S. Okuda, Phys. Stat. Sol. (a) 132 (1992) 79.
[12] H.-R. Sinning, Phys. Stat. Sol. (a) 140 (1993) 97.
[13] H. Mizubayashi, M. Shibasaki, S. Murayama, Acta Mater. 47 (1999) 3331.
[14] T. Zhang, A. Inoue, T. Masumoto, Mater. Trans., JIM 32 (1991) 1005.
[15] M. Matsumoto, H. Mizubayashi, S. Okuda, Acta Metall. Mater. 43 (1995) 1109.
[16] R. Kirchheim, F. Sommer, G. Schluckebier, Acta Metall. 30 (1982) 1059.
[17] R. Kirchheim, Acta Metall. 30 (1982) 1069.
[18] R. Kirchheim, W. Kieninger, S.Y. Huang, S.M. Filipek, J. Rush, T. Udovic, J. Less-Common Met. 172/174 (1991) 880.
[19] V.A. Khonik, L.V. Spivak, Acta Metall. 44 (1996) 367.